

EXPERIMENTAL STUDY OF THE BEHAVIOR OF NACA 0009 PROFILE
IN A TRANSONIC LEBU CONFIGURATION*

J.P. BONNET, J. DELVILLE and J. LEMAY^o

Centre d'Etudes Aérodynamiques et Thermiques, Univ. de Poitiers
Laboratoire d'Etudes Aérodynamiques, UA du CNRS 191
43 rue de l'Aérodrome- 86000 Poitiers - France

^o Permanent adress: Dept. de Génie Mécanique
Université Laval
Québec - Canada

ABSTRACT

A parametric experimental study of a LEBU in a transonic turbulent boundary layer is performed with a NACA 0009 manipulator made of composite material. The free stream Mach number varies from 0.7 to 0.8, the chord Reynolds number of the LEBU is of the order of 1.5×10^5 . The manipulating device, of chord length of the order of the incoming turbulent boundary layer thickness, is placed at variable distances from the wall with angles of attack lying between -1° and $+1^\circ$. The drag of the manipulator is measured by means of a specially designed balance. The pressure distributions on the wall beneath the LEBU are also measured. The measurements show that this kind of device has a right mechanical behavior in transonic flow. The drag of the manipulator appears higher than the usual value known for subsonic laminar situations. It appears that minimum drag occurs when the LEBU is located at a distance from the wall of the order of 70% of the boundary layer thickness. This value corresponds to the usually admitted range of distances for net drag reductions in subsonic flows. The drag is very sensitive to the angle of attack of the LEBU, the less critical position being at 50% of the boundary layer thickness. Important critical Mach numbers effects are observed for several configurations. The wall pressure distribution beneath the LEBU exhibits large negative peaks for negative angles of attack, with a particular behavior in the vicinity of the LEBU leading edge. Positive or null incidences less influence the wall pressure. All these results are compared with subsonic ones and show some specific behaviors which have to be consider.

Nomenclature

- C Chord length of the manipulator,
- Cd Drag coefficient. $Cd = D / (1/2 \rho U^2 . C . L)$
- Cp Wall pressure coefficient. $Cp = (Pw - Pq) / (1/2 \rho U^2)$
- D Streamwise component of the manipulator drag.
- L Span of the manipulator inside the test section.
- M Mach number.
- Pt Settling chamber pressure.
- Pw Wall static pressure.
- Rc Reynolds number based on the chord length of the manipulator.
- U Local streamwise mean velocity at the leading edge location of the manipulator for natural boundary layer.
- X Streamwise wall coordinate underneath the manipulator, starting beneath the leading edge of the device (see Fig. 1).
- y Coordinate normal to the wall (y=0 at the wall)
- Y Distance from the wall of the manipulator leading edge (see Fig. 1).
- α Angle of attack of the manipulator (see Fig. 1).
- δ Conventional thickness of the unmanipulated wall boundary layer (based on $U = .99 U_\infty$) at the location of the leading edge of the LEBU.
- δ^* Displacement thickness.
- θ^* Momentum thickness.
- ρ Density.

Subscript:

- ∞, e Free stream conditions.

I. INTRODUCTION

Among several solutions investigated for drag reduction in turbulent boundary layers, passive methods have been recently studied in details for subsonic, incompressible flows (see for example ^{1, 2, 3}). Inner or outer devices can be used for altering in some sense the turbulent structure of the boundary layers. In the case of inner manipulators, also called "riblets", the wall region of the boundary layer is modified by changing the wall geometry. The shape of the groves imposed to the wall seems now well optimized and have been extended with some success to transonic configurations in wind tunnel tests (³) and some supersonic flight tests are scheduled at NASA Dryden for example (⁴).

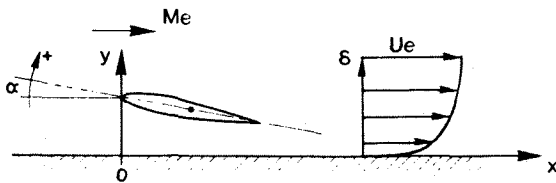


Figure 1. Coordinate System

* This study was supported by AIRBUS INDUSTRIE contract AI/TT-1 monitored by Mr. J.P. Robert.

In the case of outer manipulators, also historically called "LEBUs", the large scale structure of the turbulent boundary layer is altered by placing small blades parallel to the wall at an optimized distance from the wall which depends on the flow characteristics. Single manipulators can be used, but, at least for incompressible flows, two LEBUs mounted in tandem are generally preferred. For subsonic flows, a large number of both theoretical and experimental works have been devoted to the subject (see ² to ¹⁸ and ²⁰ to ²⁸); measurements have shown that optimized configuration of single manipulators leads to large decrease (of order of 10 to 15%) of skin friction coefficient (see for example Lemay et al. ¹⁶ or Mumford et al. ²⁰). In this case the consensus generally admitted is that the chord length of the manipulator should be of the order of the local boundary layer thickness, δ , and the device should be placed at distances from the wall lying around 0.5 to 0.8 δ . The net drag reduction which can be hoped for such manipulations is the balance between the benefit observed at the wall and the drag of the manipulator itself. It immediately follows that the shape of the manipulator should be optimized for the point of view of its own drag. For subsonic flows, Lemay et al. ¹⁶ have shown that the skin friction behavior on the wall is nearly independent of the manipulator shape (thin flat plate or thick, rectangular section blades or NACA 0009 profiles). In such flows, very thin flat blades of thickness of about 0.005 times the incoming boundary layer thickness appear to be efficient for net drag reduction. Moreover, in transonic regimes, i.e. closer from flight conditions, it is clear that flat plates can be used no longer: mechanical vibrations cannot be avoided and the elasticity of steel blades is too large to impose stable positioning inside the boundary layer. Then it appears that if LEBUs are to be used for turbulent drag reduction on aircrafts, properly shaped devices should be used. One should notice that the first LEBU flights tests were conducted by Betelrud in Sweden. His group was using thick ribbons with rounded noses and sharpened trailing edges. Despite the fact that, due to high device drag, no net drag reduction was observed, very encouraging results were obtained. As an example, LEBUs worked well up to Mach number of 0.8, with severe angle of device sweep (up to 40°, Betelrud et al. ⁵), and skin friction of the same order than incompressible results were observed.

Thus, it appears that device drag should be studied and reduced in order to lead to net drag reduction, particularly for transonic flows. The manipulator, when placed inside turbulent boundary layers, works in intricate conditions. Between all these conditions, let us recall some particular characteristics: - Turbulent incoming flow "seen" by the manipulator, leading to instationary effects (Katzmayer effect, see for example ⁵), and eventually premature transition of the boundary layers on the LEBU. These two effects can either decrease or increase the device drag; indeed they are present for subsonic configurations as well as for transonic flows, but in this last case they can have crucial influence on the compressibility effects like shock developments, wave drag, separation, etc... - Wall proximity due the fact that the manipulator is placed at a distance from the wall of the order of

its own chord length. Particularly in transonic flows, this characteristic can be predominant, and some sonic nozzle effects between the wall and the LEBU can be present and should be avoided. - The effect of the critical Mach number, inducing large sensitivity to the incidence of the manipulator and large increase of the total drag of the LEBU.

Within these experimental conditions, the optimization of the shape of airfoils used for LEBU tests is difficult from a computational point of view. Experimental results are needed as well for providing conventional shapes qualifications as for providing data which can be used for computational purposes.

In a previous study, Govindaraju and Chambers ¹³ have measured the drag of one single ribbon and tandem configuration in an incompressible turbulent boundary layer. Their results show that, in the case of a single manipulator, the drag of the thin ribbon is higher than laminar skin friction by up to 7%. The influence of ribbon location is rather low. The drag is on the other hand strongly influenced by its incidence relative to the wall at the higher chord Reynolds number (i.e. 25,000). As an example, the drag can be increased by up to 60% for an angle of attack of only 1°.

The purpose of this paper is then to perform an experimental study of the drag of a manipulator placed inside a transonic turbulent boundary layer. The LEBU is a NACA 0009 profile and the free stream Mach number of the flow can be adjusted between 0.7 and 0.8. We focus our attention on the drag of the manipulator itself, which appears to be an unavoidable first step for obtaining net drag reductions with this kind of device. Mean wall pressure field is also analysed for several configurations: height, angle of attack of the LEBU and external Mach number are varied.

II. EXPERIMENTAL ARRANGEMENT

II.1 Wind tunnel.

A closed loop blowdown wind tunnel with a maximum running time of one minute is used and schematically described in Fig. 2. For the present studies the usual running time is of the order of 20 to 30 seconds. All the experiments presented here correspond to constant total pressure and temperature, respectively 9×10^4 Pa and $300 \text{ K} \pm 10\text{K}$. The wind tunnel is driven by a supersonic ejector (Mach number 6). During the runs the temperature variations does not exceed more than 1%, due to the use of a heat exchanger in the circuit. The Mach number of the transonic flow is adjusted by positioning a flap downstream of the test section (see Fig. 2) allowing to fix a sonic nozzle of given section.

II.2 Test section.

The test section is of 1.7 m long and 150mm x 150mm of cross section. The lower wall is used as the test plate and is equipped with 95 static pressure taps of 0.5 mm in diameter. These taps are located from 15 mm upstream of the leading edge of the manipulator up to 450 mm downstream. The upper wall of the wind tunnel is adjustable in order to either set the zero pressure gradient (present experiments) or give

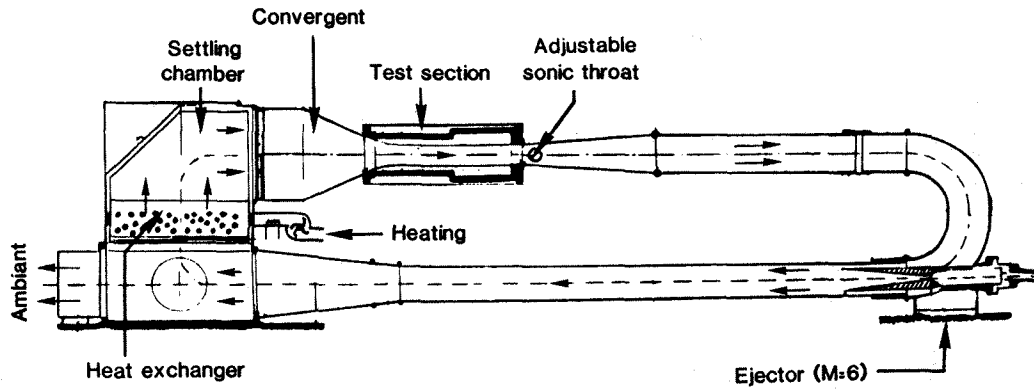


Figure 2. Schematic of the Transonic Wind Tunnel

some prescribed wall pressure distribution. The static pressure evolution for the natural (unmanipulated) boundary layer, shown on Fig. 3, indicates that the top wall is well adjusted to provide negligible pressure gradient.

At the entrance of the test section, 20 mm wide sand paper strips are stuck on both upper and lower walls in order to obtain fully developed boundary layers at the location of the manipulator. The LEBU leading edge is then located 500mm downstream of the tripping device, the local Reynolds number being there of the order of 5×10^5 . The length of the wall observed downstream of the LEBU is then of 440 mm and the sonic throat is located at 550 mm from the leading edge of the manipulator.

The side walls of the test section are equipped with windows allowing to perform some stroboscopic visualizations. Thin slots, 3 mm thick and 20 mm long, are machined in these windows in order to pass the manipulator through without any mechanical contact.

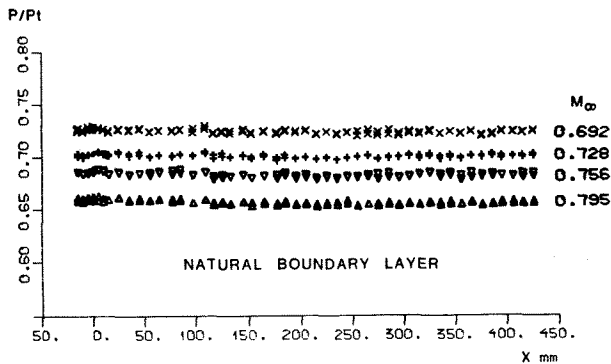


Figure 3. Distribution of Wall Static Pressure in Natural Boundary Layer

II.3 Manipulator tightening device.

The apparatus described in Fig. 4 enables to set the manipulator at any angle of attack with respect to the wall, for heights varying from the wall up to $Y = 13$ mm.

A specially designed, light support made of dural is used to tighten the manipulator. The longitudinal strength imposed to the LEBU is applied by two screws located at both ends of the support where the manipulator is fastened. The applied stress is deduced from the stretch,

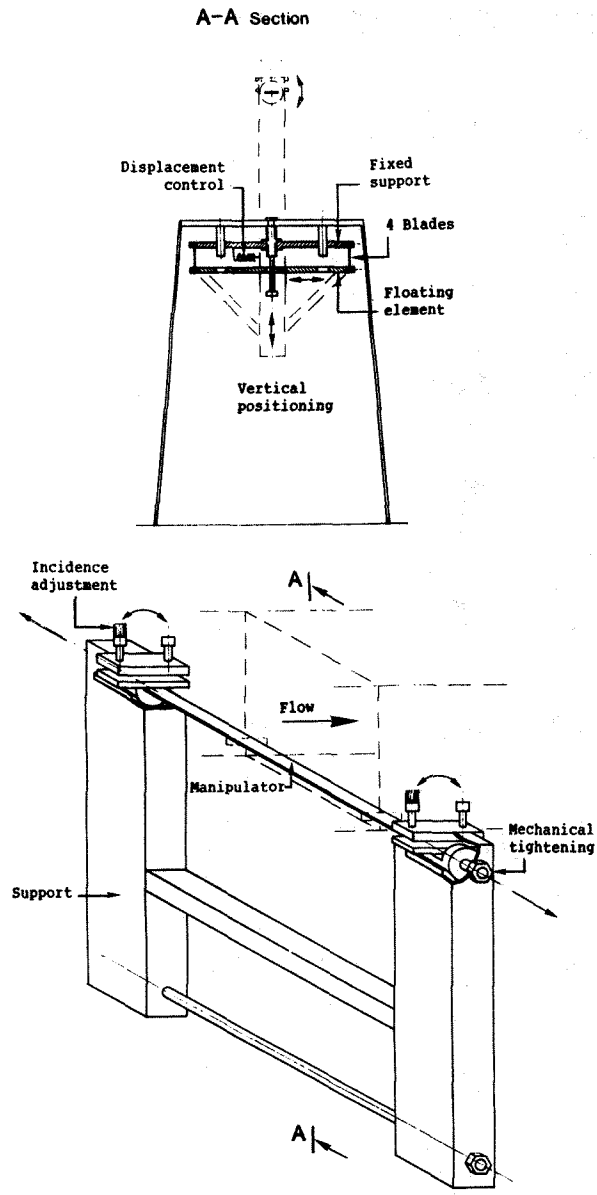


Figure 4. Schematic of the LEBU Drag Balance

measured by two micrometers, associated with a calibration curve independently provided by a traction tensile strength test (see section II.5).

The angle of attack is adjusted by micrometric screws associated with a precision spirit level put on a reference surface located on the LEBU fastening mechanism. A complementary check is performed with a micrometer measuring the manipulator position relative to the wall of the test section.

In order to let the LEBU free to move in the slots described in section II.2, a special apparatus has been designed, allowing to isolate the device from wind tunnel vibrations and to avoid pressure losses: an external box, including the whole mechanism of mechanical positioning, tightening and drag balance, is installed in connection with muffles. These muffles are stuck on the external glasses of the test section. For each experiment, the data acquisition starts after 10 seconds of run, this time corresponds to the measured emptying duration of the box and ensures pressure equilibrium.

During each test, the evolution of the position of the LEBU is controlled by reflecting a laser beam (HeNe) on the device. The displacements of the beam are checked at a distance of 2 meters. In order to avoid misinterpretations of the observations, the spanwise location of the impinging of the beam on the profile is a non entire fraction of the full span. Several tests are also performed by varying the location of this point.

II.4 Drag balance device and calibration.

The moving assembly described in section II.3 is hung on a fixed support (Fig. 4) by a pantograph type system. Four steel blades, 0.2 mm thick, 10 mm wide and 20 mm long, are associated to an hydraulic damping device; this system provides a mechanical couple balancing the drag of the LEBU following the direction parallel to the wall. The drag measurement is then obtained by measuring the displacement of the moving support which is detected by a Linear Variable Differential Transformer (LVDT). This kind of sensor allows direct estimation of the force applied on the LEBU in term of the LVDT output voltage. We use a simple calibration procedure described in Fig. 5: given efforts are imposed to both ends of the LEBU lying outside of the test section by an arrangement of wires put at a precisely defined angle and tightened by calibrated weights.

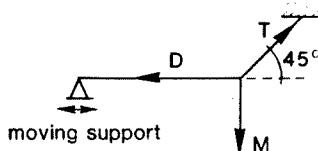


Figure 5. Calibration Procedure of Drag Balance

Several tests have shown that the system gives a quite linear and well reproducible response in the 0-2 Newtons range, which corresponds to the usual range of the present experiments. The damping of the system is adjusted in accordance to response time compatible with the run durations. We have observed that this system is sensitive to zero drifts which are systematically measured. The estimated accuracy of

the whole system is evaluated to be better than 5%.

II.5 Manipulator characteristics.

The manipulator tested in this study is a NACA 0009 profile of 12.7 mm in chord length. The total span is 193 mm, exceeding the span of the test section. The LEBU is made from casting carbon fibers around an inner steel blade.

Tensile stress tests have shown that the breaking occurs for a traction strength of 6,500 N. In order to remain within the elastic domain of this composite material, a maximum load of 4,000 N is chosen to tighten the LEBU. This corresponds to an increase of length of 0.62 mm which is the reference in the present experiments and provides repeatable mechanical tightening. After each series of runs, the manipulator is unloaded in order to avoid useless stress.

II.6 General instrumentation.

The total temperature T_g is measured inside the settling chamber by a Chromel-Alumel thermocouple of 0.32 mm in diameter, connected to a ZEREF cold reference regulated within 0 ± 0.05 Celsius degree.

The total pressure P_g is also measured in the settling chamber by a total pressure probe. This probe, altogether with the 48 selected static pressure taps are connected to Bell & Howell pressure transducers. Scanning technique is applied for the wall pressure taps.

Total pressure traverses through the boundary layer are performed by a tube of inner diameter of 0.5 mm (outer diameter 0.7 mm) connected to one of the pressure transducers.

All the analogical outputs (pressures, temperature and drag balance) are amplified and digitized by a CAMAC system controlled by a Matra-Datasystem 100/550 mini-computer

III. RESULTS

III.1. Flow characteristics.

All the experiments are performed for four free stream Mach numbers, respectively $M_\infty = 0.7, 0.72, 0.75$ and 0.8 . The value imposed to the section of the sonic throat is not perfectly identical from one adjustment to the other. A maximum variation of M_∞ of 0.01 is observed and corresponds to 1.5% in term of relative variation.

The chord Reynolds number of the manipulators lies between 1.4×10^5 and 1.6×10^5 depending on the free stream Mach number and the location inside the boundary layer. The table 1 presents the overall characteristics of the different configurations studied.

The mean velocity profiles in the boundary layers in the absence of the LEBU and corresponding to $X = 0$ are plotted on Fig. 6. The integral parameters measured for the four Mach conditions are also given in table 1. These values are obtained following the usual compressible formula, see for example Mathews et al., without any correction for wall proximity, turbulence level, etc... The main properties of these boundary layers appear to be in agreement with well known characteristics of fully developed turbulent boundary layers without pressure gradient.

Me = 0.70

$\delta = 11.0$ mm; $\delta_1/\delta = 0.123$; $\theta/\delta = 0.090$

Y (mm)	Y/δ	M	$\rho U^2/2$ (Pa)	Rc
12.5	1.14	0.700	2.25E+04	1.50E+05
9.2	0.84	0.698	2.24E+04	1.50E+05
7.2	0.65	0.687	2.19E+04	1.49E+05
5.2	0.47	0.686	2.19E+04	1.49E+05
4.2	0.38	0.646	2.01E+04	1.43E+05
3.2	0.29	0.623	1.90E+04	1.40E+05
2.2	0.20	0.592	1.76E+04	1.35E+05

Me = 0.72

$\delta = 10.6$ mm; $\delta_1/\delta = 0.127$; $\theta/\delta = 0.091$

Y (mm)	Y/δ	M	$\rho U^2/2$ (Pa)	Rc
12.5	1.18	0.720	2.34E+04	1.53E+05
9.2	0.87	0.715	2.32E+04	1.52E+05
7.2	0.68	0.707	2.28E+04	1.51E+05
5.2	0.49	0.677	2.15E+04	1.47E+05
4.2	0.40	0.660	2.07E+04	1.45E+05
3.2	0.30	0.634	1.95E+04	1.41E+05
2.2	0.21	0.598	1.79E+04	1.36E+05

Me = 0.75

$\delta = 10.1$ mm; $\delta_1/\delta = 0.125$; $\theta/\delta = 0.090$

Y (mm)	Y/δ	M	$\rho U^2/2$ (Pa)	Rc
12.5	1.24	0.750	2.47E+04	1.57E+05
9.2	0.91	0.743	2.44E+04	1.56E+05
7.2	0.71	0.735	2.40E+04	1.55E+05
5.2	0.51	0.703	2.26E+04	1.51E+05
4.2	0.42	0.681	2.17E+04	1.48E+05
3.2	0.32	0.659	2.07E+04	1.45E+05
2.2	0.22	0.623	1.90E+04	1.40E+05

Me = 0.80

$\delta = 9.0$ mm; $\delta_1/\delta = 0.123$; $\theta/\delta = 0.088$

Y (mm)	Y/δ	M	$\rho U^2/2$ (Pa)	Rc
12.5	1.39	0.800	2.67E+04	1.62E+05
9.2	1.02	0.795	2.65E+04	1.62E+05
7.2	0.80	0.781	2.60E+04	1.60E+05
5.2	0.58	0.754	2.48E+04	1.57E+05
4.2	0.47	0.728	2.37E+04	1.54E+05
3.2	0.36	0.703	2.26E+04	1.51E+05
2.2	0.24	0.662	2.08E+04	1.45E+05

- Table 1 -

III.2. Preliminary observations.

Drag measurements have been performed for the four free stream Mach numbers, and for the following positions of the manipulator relative to the wall: Y= 2.2, 3.2, 4.2, 5.2, 7.2 and 12.5 mm. For each configuration, the incidence of the LEBU was adjusted to $\alpha = -1, 0$ and $+1$ degree. Intermediate values, $\alpha = -0.5$ and $+0.5$ degree are also given at Y=12.5 mm, i.e. near the outer frontier of the boundary layers.

All the angles of attack are adjusted in the absence of the flow, and determined by coupling position measurements using precision micrometers and spirit level. During the runs, we check the modifications of the angle of incidence by the observation of the deflexion of the laser beam using the arrangement described in section II.3. The initial positioning is very slightly affected when the wind tunnel is running, and the maximum variation of the initial angle is always less than 0.1 degree, excepted for the closest distance from the wall (Y=2.2 mm) when the Mach number is high (M= 0.75 and 0.8). As a comparison we can notice that some trials performed with thin

steel blades (square section with thickness 0.1 mm) exhibits large parasitic incidence modifications associated with large amplitude vibrations appearing over several modes. The profiles used in this study doesn't show noticeable vibrations, excepted the abovementioned configuration.

The very good stability of the LEBU used is a quite favourable characteristic for the use of composite materials; the thickness of the profile appears to be sufficient to prevent parasitic and prohibited for drag reduction-vibrations or deformations.

We give in table 1 the main characteristics of the set of experiments: local Mach number, mass flux and Reynolds number.

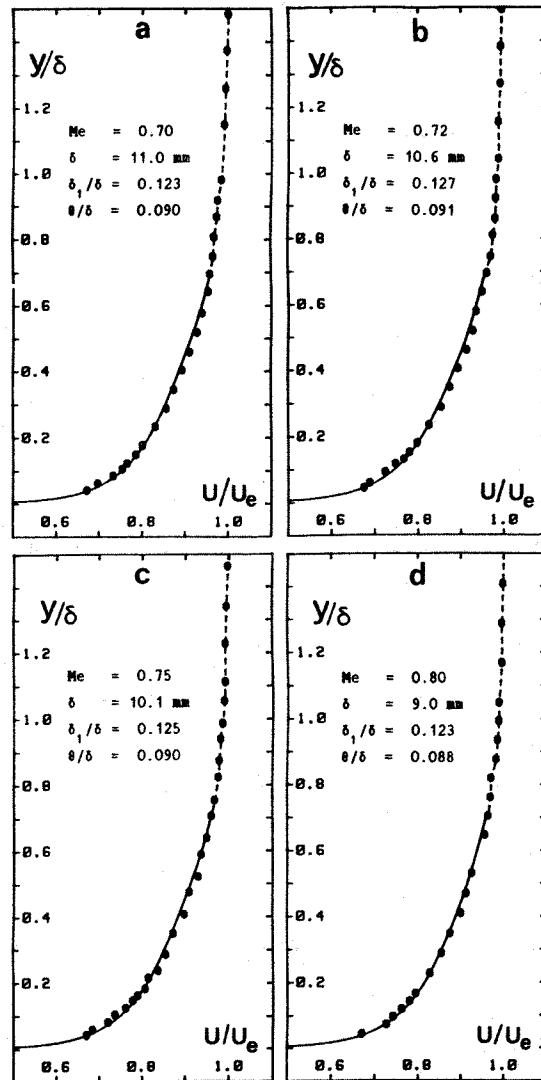


Figure 6. Mean Velocity Profiles in Natural Boundary Layer

III.3. Drag measurements

Figure 7 presents the evolution of the direct drag measurements of the NACA 0009 profile placed without incidence for several positions relative to the wall.

The absolute value of the drag is of interest if the balance of profile drag and wall skin friction are to be considered: the net drag reduction or increase associated to a given configuration is the result of the wall skin friction reduction (not evaluated here) due to LEBU effect and the drag of the manipulator itself. Then it will be important to choose a configuration minimizing the drag of the manipulator, this configuration being coherent with the optimum wall skin friction reduction.

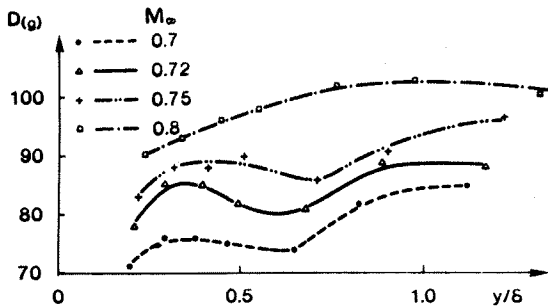


Figure 7. Evolution of LEBU Drag vs Y at Zero Angle of Attack

We can observe in Fig. 7 that, for free stream Mach numbers less than 0.8, minima of direct drag are present and correspond to Y locations lying between 0.3 and 0.7xδ. These positions are in the area of optimum Y locations for skin friction reduction observed for subsonic flows (see for example ¹⁶, ²⁰ or ²⁴). This is a very encouraging first result. For higher Mach number, $M_{\infty}=0.8$, a continuous increase of the drag is observed, associated as expected to a higher absolute value.

Even if the drag of the manipulator is of direct interest for net drag balance, the observation of the drag coefficient, C_d , is of interest in order to perform quantitative comparisons and physical interpretations. Figure 8 shows the drag coefficient behavior for the three angles of incidence α . For zero incidence, Fig. 8b), we still can observe a minimum of C_d corresponding to $Y/\delta \approx 0.7$ for M_{∞} less than 0.8. No minimum can be observed for the highest Mach number.

The mean value of C_d lies around 2×10^{-2} whatever M_{∞} is. This value is somewhat higher than the values generally reported for subsonic flow. As an example, let us recall the results of Abbot et al. ¹, giving $C_d \approx 0.93 \times 10^{-2}$ for 2% of free stream turbulence level and 0.87×10^{-2} for 0.08%, at nearly the same Reynolds numbers but at lower speeds. As a comparison, the laminar skin friction on both sides of the profile evaluated from the usual Blasius formula gives a C_d value of the order of 7×10^{-3} . It then appears that the NACA 0009 profiles have here nearly twice the optimal drag coefficient measured for subsonic, laminar conditions.

It should be noticed that the profiles used for all LEBUs studies are placed in quite unusual situations:

The external turbulence level "seen" by the wing is high, even for the largest distances from the wall tested here. Some transitional effects cannot be avoided, but these effects can be partially compensated by the Katzmayer effect due

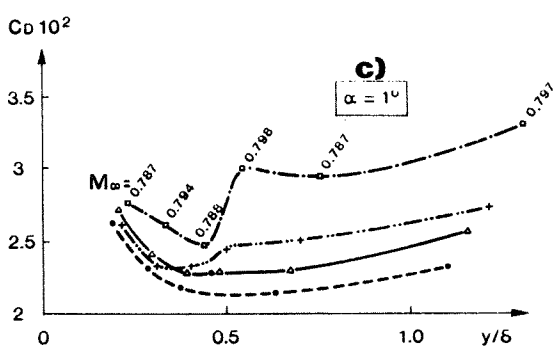
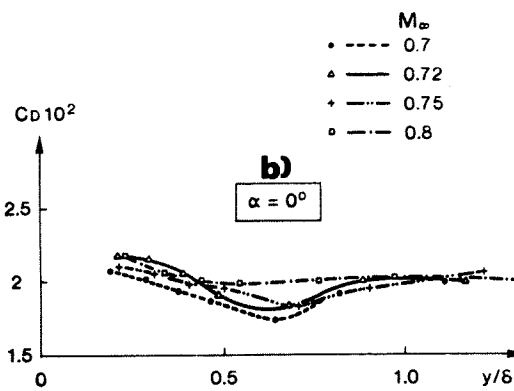
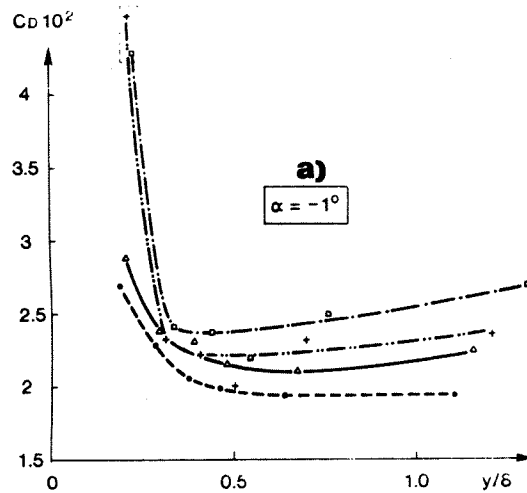


Figure 8. Evolution of LEBU Drag Coefficient vs Y for: a) $\alpha = -1^\circ$; b) $\alpha = 0^\circ$; c) $\alpha = 1^\circ$

to the associated fluctuations of instantaneous incidence angles (Bertelrud and Watson⁵).

The wall proximity can influence the drag of the profiles. The maximum distance from the wall is at maximum of the order of the chord length of the profile.

The relative surface roughness of the manipulator is quite difficult to determine. Although the surface, from the building process looks very smooth, the small size of the model can lead to non negligible relative roughness and then can contribute to the observed increase of drag coefficient by premature transition.

All the abovementioned effects can be additive, leading to the relatively large drag coefficient observed.

When the LEBU has a negative incidence in the flow, Figure 8a) shows practically no minimum value. However, for locations close to the wall ($Y/\delta < 0.3$), we can observe large increase of C_d , due to important vibrations for Mach numbers of 0.75 and 0.8. These Y locations of the LEBU are quite unrealistic from the general point of view of net drag reduction. But, during the different flying regimes of airplanes, the size of the boundary layers are subject to considerable modifications; then, if LEBUs are to be installed, their height relative to the wall will be constant and the observation of non optimized characteristics is of interest.

For negative angles of incidence, it appears one more time that, for manipulator drag, the optimal Y location is about 0.76.

For positive incidence angles (Fig. 8c), a strong increase of C_d is observed for $M_\infty = 0.8$. The apparent chaotic behavior observed for this Mach number can be explained by some small variations of the value of M_∞ for one experiment to another. As previously mentioned, the Mach number is adjusted by pivoting a flap in order to vary the section of the sonic nozzle. Since this flap cannot be set exactly at the same position among the different runs, variations of M_∞ of the order of 0.01 are observed. The corresponding Mach numbers are reported on the curve in Fig. 8c). Taking into account the great sensitivity to the Mach number for these incidence angles, the large variations of C_d can be understood. This last point will be discussed later in more detail.

Figure 9 shows the evolution of C_d for each Y position according to the free stream Mach number value and the angle of attack. The local values of the Mach number are given on the figures. The greater incidence sensitivity is observed when the manipulator is placed near the external part of the boundary layer, typically for $Y = 7.2$ and 12.5 mm (corresponding to $Y/\delta \approx 0.8$ and 1.4), and for the highest Mach numbers. This effect clearly corresponds to the critical Mach number effect.

From the observation of Fig. 9, it appears that the better location of the LEBU compatible with the maximum skin friction reduction configuration given by several authors corresponds to $Y = 5.2$ mm, i.e. $Y/\delta \approx 0.5$. Indeed, for this position, the drag sensitivity to the angle attack seems to be the lower one. However, for this location, positive angles of attack should be avoided in order to bypass critical Mach number effects.

Figure 10 shows the influence of the Mach number obtained just outside of the boundary layer, $Y/\delta < 1.4$. For zero incidence, the Mach number has no noticeable influence on the drag coefficient. On the contrary, for small positive or negative incidences, $\alpha = \pm 0.5$ degree, the drag coefficient increases, mainly for positive angles. This result shows that the critical Mach number is quite close to 0.8 within the present experimental conditions. The usual critical Mach number given in the literature lies under this value, i.e. 0.76.

From Fig 9 and 10, one can observe that the zero reference of the incidence corresponds to the minimum of C_d , confirming the very small evolution of the positioning of the manipulator observed during the runs by the laser-beam technique described above. Excepted for the locations very close to the wall -and unrealistic

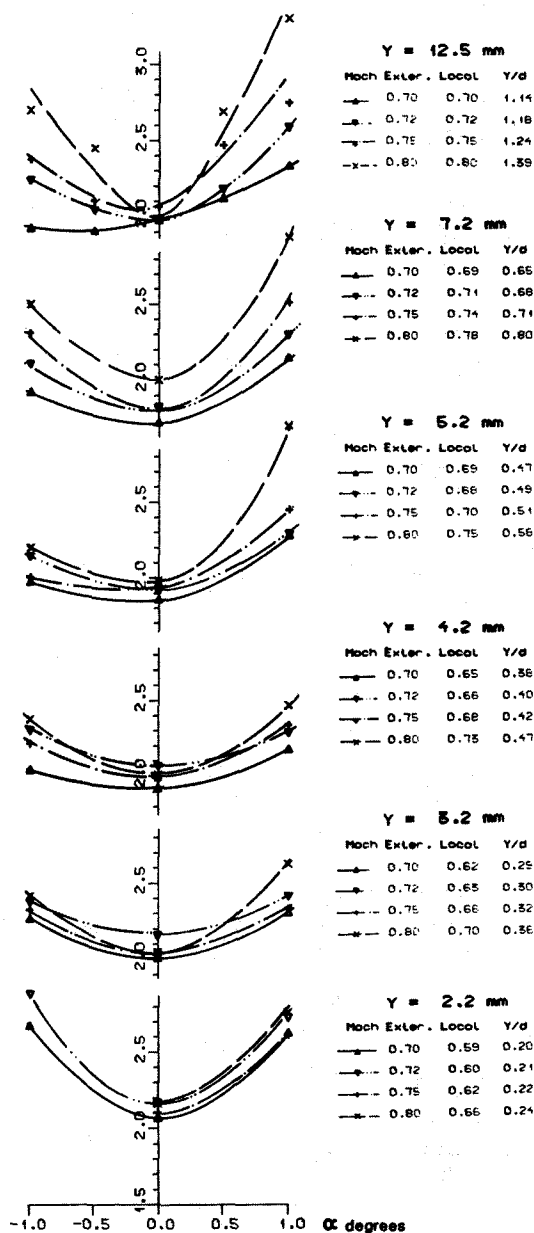


Figure 9. Evolution of LEBU Drag Coefficient vs α for Several Y

from the point of view of net drag reduction- the positive incidences for $Y > 5.2$ mm have a more dramatic effect when compared to negative ones (Fig. 9). These different behaviors will be discussed later in terms of wall pressure distributions.

Very close to the wall ($Y = 2.2$ mm), negative incidence have dramatic effects on the drag for free stream Mach numbers greater or equal to 0.75 because strong vibrations are present, increasing the drag and might be damaging the manipulator.

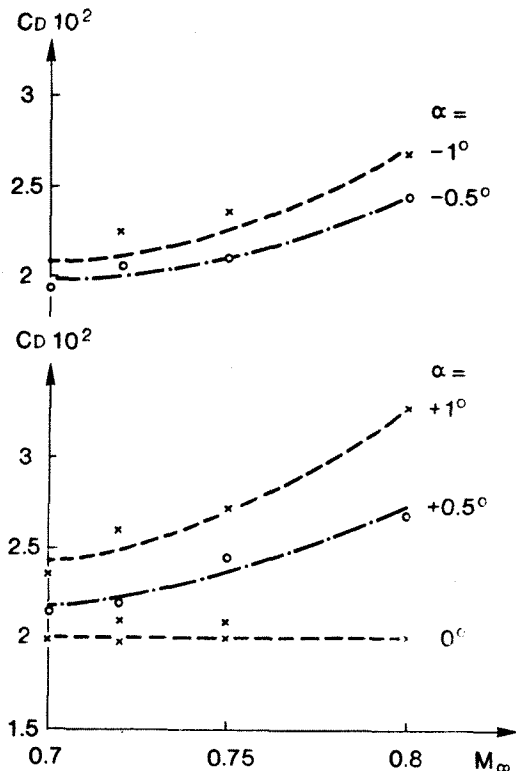


Figure 10. Evolution of LEBU Drag Coefficient vs Free Stream Mach Number Outside of the Boundary Layer

We plot on Fig. 11 the evolution of the drag coefficient obtained at constant local Mach number, equal to 0.7. Then, the only varying parameters are the wall proximity (Y/δ varies from 0.36 to 1.14) and the local turbulence level "seen" by the manipulator. We can observe that the overall behaviors of C_d versus angles of attack are quite similar, with a previsible increase of the level when the LEBU approaches the wall. The result shown for $M_\infty = 0.7$ and $Y = 7.2$ mm exhibits a loss of symmetry which can be related to an ill initial angular positioning, the error being less than 1 degree.

The sensitivity to incidence angle appears to be quite unaffected by the location inside the boundary layer, and therefore the Mach number seems to be the relevant parameter for this point of view.

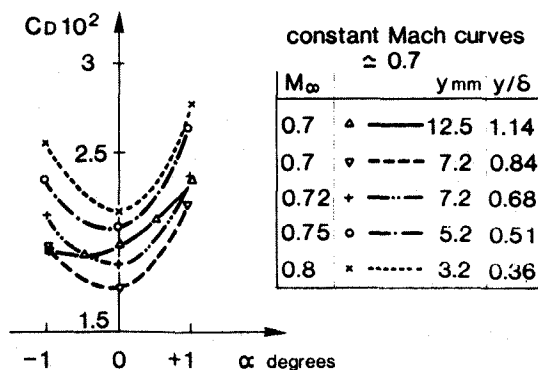


Figure 11. Evolution of LEBU Drag Coefficient vs α at Constant Local Mach Number

III.4. Pressure distribution beneath the device.

Figure 12 shows an example of the entire streamwise extent of the measured wall pressure beneath the device, non-dimensionalized by the pressure in the settling chamber. We can observe that the wall pressure is only affected in a restricted region corresponding to the immediate vicinity beneath the LEBU. The upstream (undisturbed) wall pressure is recovered at about 30 mm downstream the leading edge of the manipulator, corresponding to about 3 δ .

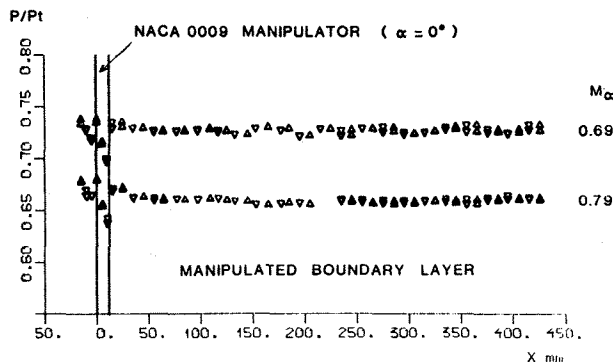


Figure 12. Example of Static Pressure Distribution on the Wall beneath the LEBU

We plot on Fig. 13 the wall pressure distributions from $X = -15$ mm up to $X = 45$ mm, corresponding to -1.5δ and 4.5δ . These results are also plotted in term of the pressure coefficient, C_p .

For zero incidence, the modifications of the wall pressure are mainly observed immediately below the LEBU. The influence of the free stream Mach number seems quite low, but, as expected, the C_p variations are strongly influenced by the location of the manipulator inside the boundary layer. When the LEBU is far from the wall, one observe a small increase of C_p followed by negative values at approximately 80% of the chord length of the LEBU, C_p remaining always greater than -0.1 . When the LEBU approaches the wall, still for $X/\delta \approx 0.8$, the observed minimum values of C_p reaches -0.2 .

Some of these results can be compared with the experimental data and inviscid calculations of Bandyopadhyay and Watson. These authors use also NACA 0009 profiles with nearly the same geometrical configuration but for low velocities. Figure 14b) compares the present results obtained for the extreme values of M_∞ (0.6 and 0.8) with the experiments and the inviscid calculations in incompressible regime for the closest characteristics: $C/\delta \approx 1.1$ and $Y/\delta \approx 0.8-0.9$. The comparison between incompressible and transonic regimes shows that the orders of magnitudes of C_p are comparable. However, the main difference appears at the wall location corresponding to the leading edge of the LEBU ($X/C = 0$). Unfortunately, the experimental arrangement doesn't allow to give more detailed measurements in the immediate vicinity of the leading edge position. However, we can observe that the corresponding pressure tap cannot be directly accused, because in the natural boundary layer the

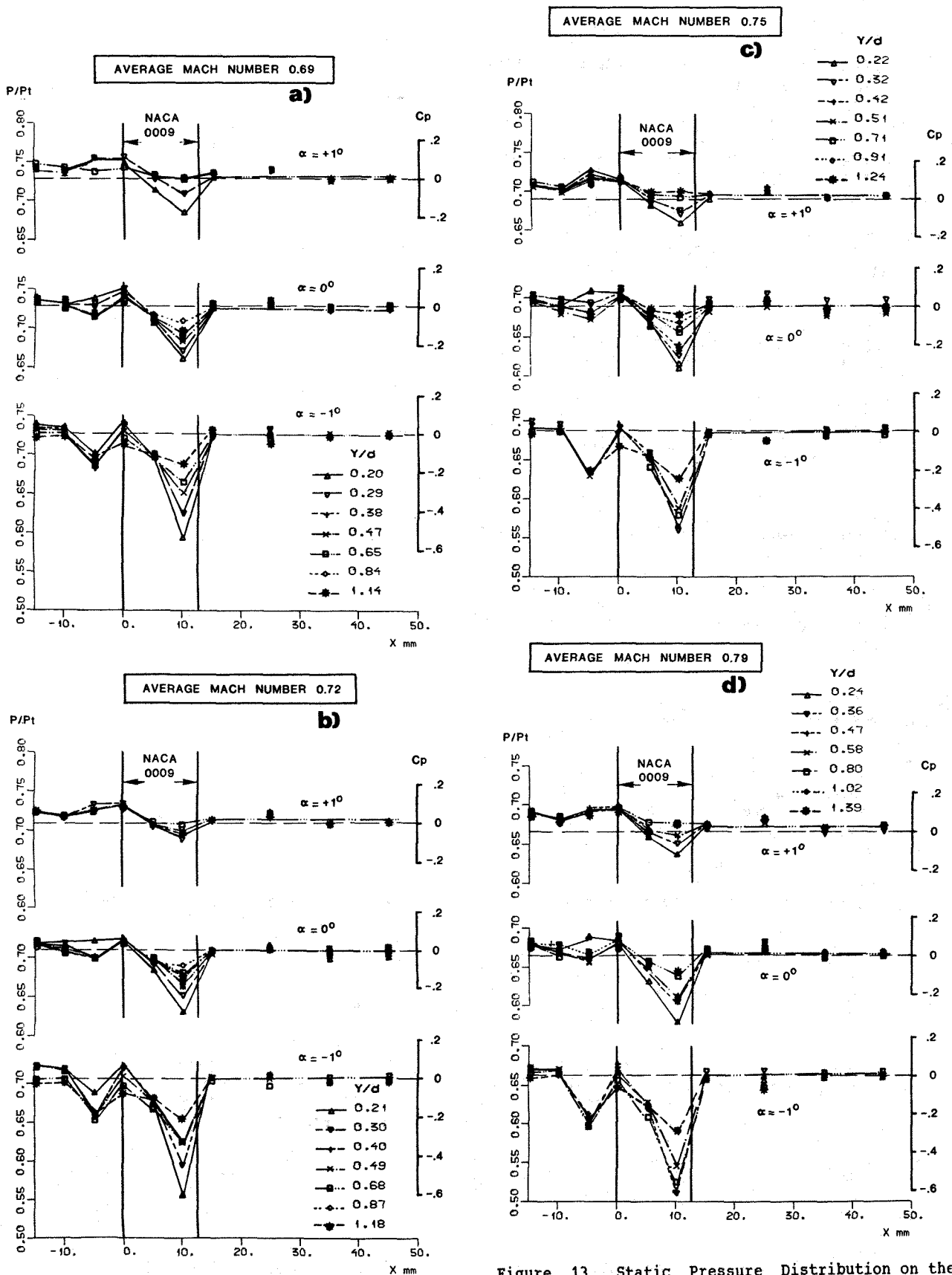


Figure 13. Static Pressure Distribution on the Wall beneath the LEBU in the Vicinity of the Manipulator. a) $Me = 0.69$; b) $Me = 0.72$; c) $Me = 0.75$ and d) $Me = 0.79$

results are consistent with the neighbouring points, and the pressure measured at this point evolves in a satisfactory manner when the Mach numbers varies. So, it appears that, for compressible flows, the LEBU induces strong perturbations of the wall pressure just beneath its leading edge, even for zero incidence. This kind of behavior is not detected or calculated for comparable subsonic configurations.

When negative angles of attack are imposed to the LEBU, the wall "sees" the suction side of the manipulator with associated strong negative C_p values. Figures 13 clearly shows the effect of the manipulator. As for zero incidence, the position on the wall corresponding to the leading edge of the LEBU is subject to rapid increase of C_p , and the unmanipulated value is reached at $X = 0$. We can observe from these figures that the modifications of the wall pressure upstream of the manipulator seems to remain practically unchanged when both the position of the LEBU is modified and the free stream Mach number evolves from 0.7 to 0.8. The first minimum is observed for $X/\delta \approx -0.5$ and lies around -0.2. On the contrary, the minima observed just behind the manipulator are quite dependant of the Y position of the LEBU.

For these negative values of α , the comparison with the work of Bandyopadhyay and Watson in incompressible flow is more complicated. Indeed, these authors have not tested the $\alpha = -1^\circ$ situation, and our experiments does not cover the position $Y/\delta = 0.9$. Then we recall on Fig. 14a) the subsonic results obtained by Bandyopadhyay and Watson for angles of attack of 0. and -2 . degrees. The present results are interpolation between $Y/\delta = 0.8$ and 1.4, for the upper Mach number. One can observe that the transonic results show large wall pressure perturbations, of the order of 4 times the incompressible ones, but remaining of the same sign. This difference can be related to the critical Mach number value inducing large modifications of the drag and lift coefficients. Unfortunately, only the streamwise component of effort applied on the LEBU is measured here.

When positive angles of attack are given to the LEBU, the wall pressure reflects the evolution of the pressure on the pressure side of the manipulator, which is in normal conditions less strong than the one observed on the suction side.

Figure 13 shows the pressure distribution on the wall beneath the manipulator. One can observe that, excepted when the LEBU is very close to the wall, the C_p values remain positive, with small variations compared to zero or negative angles of attack.

The comparison with the experiments of Bandyopadhyay and Watson are presented on Fig. 14c). One can observe that the overall behaviors are quite similar. The transonic results appears to be of the order of magnitude of the subsonic results obtained for angles of attack of 2 degrees, i.e. twice the value of the present study. One should notice that the scale of Fig. 14c) is larger than that of Fig. 14a), the absolute maximum level of C_p measured for positive angles being of the order of 1/6 of observations for negative incidences.

For both sets of experiments (transonic or incompressible), the disturbed region on the wall is larger for positive α values than for negative ones (Fig. 14c) and 14a). When the incidence is

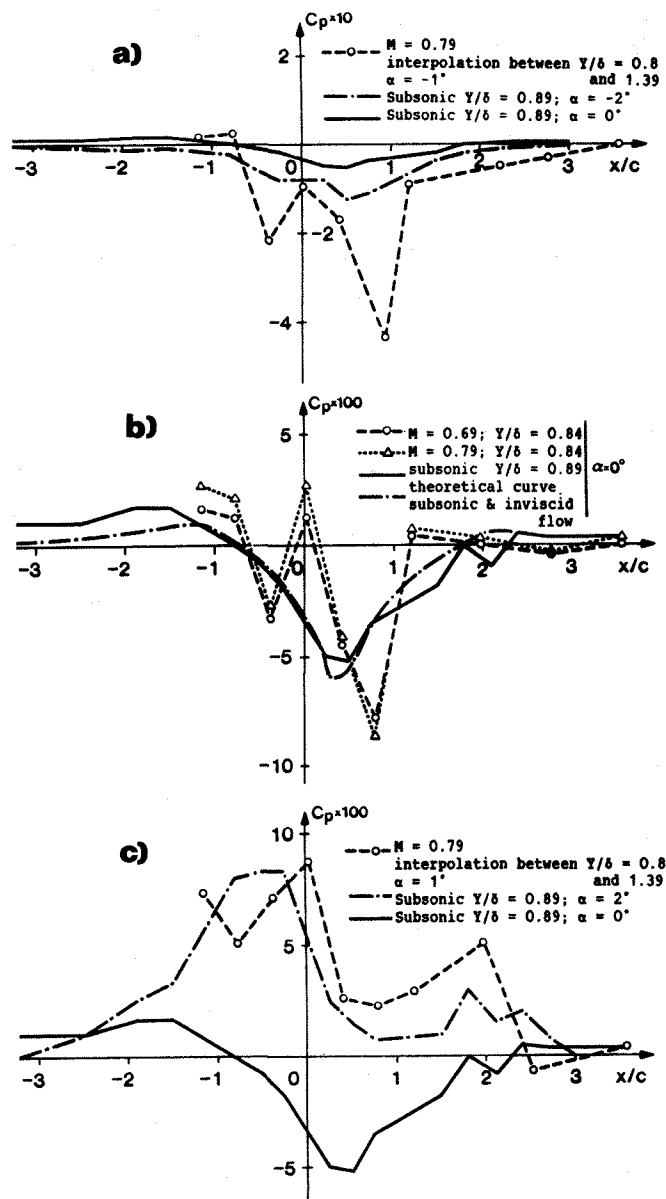


Figure 14. Static Pressure Distribution on the Wall beneath the LEBU in the Vicinity of the Manipulator. Comparison with incompressible results (*) for: a) $\alpha = -1^\circ$; b) $\alpha = 0^\circ$; c) $\alpha = 1^\circ$

positive, the main wall perturbations are observed upstream of the manipulator and extends up to about 36 upstream; the downstream perturbation is rather low but extends down to 36 as well for incompressible and transonic flows.

As for the subsonic studies performed by Bandyopadhyay and Watson, positive angles of attack seems to be beneficial from the wall pressure distribution when compared to zero or negative ones. These authors conclude from this remark that small positive incidence can be applied to symmetrical manipulators in order to achieve net drag reductions. A somewhat similar situation occurs for transonic flows. However, this possibility should be considered with care in transonic regimes, due to larger wall effects and to the strong increase of manipulator drag when the incidence is different from zero.

IV CONCLUSIONS AND PROSPECTS

The present experiments were devoted to the test of the behavior of a thin airfoil profile as outer layer manipulator for turbulent drag reduction. Emphasis has been given on the drag of the LEBU as well as on the induced wall pressure on the manipulated plate. The experiments were performed in transonic regime, for free stream Mach number lying between 0.7 and 0.8, and for Reynolds number of the manipulator being lower than those observed in usual flight conditions.

As a first conclusion, it has been demonstrated that composite material is a good solution for the mechanical rigidity of thin shapes. Providing the distance from the wall is not very small, no noticeable vibrations are detected on the LEBU.

For the NACA 0009 manipulator, the drag coefficient observed is somewhat larger than for laminar, incompressible usual results. Some specifically compressible effects are to be considered in conjunction with the particular conditions imposed to the manipulator (wall proximity, turbulence level). These effects are also present in subsonic flows but induce only a little increase of device drag. Then, the transonic regime should induce some extraneous effects increasing the drag of the manipulator itself.

In the absence of global drag measurements (taking into account both wall skin friction modifications and manipulator drag), we have tested in details the LEBU drag for several locations inside the boundary layer, angles of attack and free stream Mach numbers.

The minimum of manipulator drag is observed for distances from the wall of the order of 0.6 or 0.7 δ , for free stream Mach numbers less than 0.8. The optimum location of manipulators determined for maximum skin friction reduction in subsonic flows is close to these values.

For $Y/\delta \approx 0.6$, the manipulator drag is very sensitive to small angles of attack. At the higher Mach number, $M_\infty = .8$, this behavior is particularly noticeable. It appears that, for the NACA 0009 profile, the critical Mach number is nearly reached. For this point of view, shapes with higher critical Mach number should be preferred. Negative values of the incidence induces less device drag increase than positive ones. The results show that, as far as some variations in the angle of attack should inevitably be encountered in the real tests, the best position inside the boundary layer is $Y/\delta \approx 0.5$.

The pressure distributions on the wall beneath the manipulator show, for negative angle of attack, some particular behavior at the location corresponding to the leading edge of the LEBU. A rapid increase of the wall pressure is observed at this point and there is no comparable effects in subsonic flows. The wall pressure changes are quite larger than for comparable incompressible tests.

For zero or positive angles of attack, the wall pressure modifications due to the presence of the LEBU are less important than for negative incidences. The results obtained are closer to the incompressible ones. However, unlike for subsonic configurations, it is not evident that small positive angles of attack can be allowed for net drag reduction.

For future works, some points should be treated: first, it appears that different manipulators shapes are to be tested in such intricate situation. Calculations are needed for this purpose and the present results can serve for the validation of calculations. Then, a global study of the performance of all the drag reduction system should be performed. All these studies seem quite useful prior -or in a parallel way- to more realistic but expensive and delicate tests for example in flight conditions.

Lastly, let us recall that the question of the benefit of tandem configuration compared with single manipulator is still opened when transonic, high Reynolds numbers are considered. Then the natural extension of these wind tunnel studies should be the test of different configurations allowing to prepare larger scale tests.

Aknoledgements

The authors gratefully aknowledge Dr. V. Schmitt from ONERA Chatillon (France) for manufacturing the composite airfoil.

References

- 1 Abbot I.H., Von Doenhoff A.E. & Stivers L.S., "Summary of Airfoil Data", NACA Report No. 824, 1945.
- 2 Anders J.B., "Large Eddy Breakup Devices as Low Reynolds Number Airfoils", SAE Technical Papers Series, 1986, Paper N. 861769.
- 3 Anders J.B., Walsh M.J. & Bushnell D.M., "The Fix for Tough Spots", Aerospace America, January 1988, pp. 24-27.
- 4 Bandhyopadhyay P.R. & Watson R.D., "Pressure Field Due to Drag Reducing Outer Layer Devices in Turbulent Boundary Layers", Experiments in Fluids Vol. 5, Springer-Verlag, 1987, pp. 393-400.
- 5 Bertelrud A. & Watson R.D., "Use of LEBU-Devices for Drag Reduction at Flight Conditions", Turbulent Drag Reduction by Passive Means, R.A.S., 1987, pp. 213-249.
- 6 Blackwelder R.F. & Chang S.I., "Length Scales and Correlations in a LEBU Modified Turbulent Boundary Layer", AIAA 24th Aerospace Sciences Meeting, Reno, Nevada, January 6-9, 1986, Paper No. AIAA-86-0287.
- 7 Bogard D.G. & Coughran M.T., "Bursts and Ejections in a LEBU-Modified Boundary Layer", 6th Turbulent Shear Flows, Toulouse, September 7-9, 1987.
- 8 Bonnet J.P., Delville J. & Lemay J., "Study of LEBUs Modified Turbulent Boundary Layer by Use of Passive Temperature Contamination", Turbulent Drag Reduction by Passive Means, R.A.S., 1987, pp. 45-68.
- 9 Bushnell D.M., "Body Turbulence Interaction", AIAA 22nd Aerospace Sciences Meeting, Reno, Nevada, January 9-12, 1984, Paper No. AIAA-84-1527.

- 10 Coustols E., Cousteix J. & Bélanger J., "Drag Reduction Performances on Riblet Surfaces and Through Outer Layer Manipulators", Turbulent Drag Reduction by Passive Means, R.A.S., 1987, pp. 250-289.
- 11 Delville J., Bonnet J.P. & Lemay J., "Etude Expérimentale de l'Influence d'un Manipulateur de Turbulence de Type Lame Mince sur la Structure d'une Couche Limite Plane Incompressible", 24e Colloque d'Aérodynamique Appliquée, Poitiers, October 26-28, 1987.
- 12 Falco R.E. & Rashidnia N., "What Happens to the Large Eddies when Net Drag Reduction is Achieved by Outer Flow Manipulators", Turbulent Drag Reduction by Passive Means, R.A.S., 1987, pp. 477-510.
- 13 Govindaraju S.P. & Chambers F.W., "Direct Measurement of Drag of Ribbon Type Manipulators in a Turbulent Boundary Layer", AIAA 24th Aerospace Sciences Meeting, Reno, Nevada, January 6-9, 1986, Paper No. AIAA-86-0284.
- 14 Guezennec Y.G. & Nagib H.M., "Documentation of Mechanisms Leading to Net Drag Reduction in Manipulated Boundary Layers", AIAA Shear Flow Control Conference, Boulder, Colorado, March 12-14, 1985, Paper No. AIAA-85-0519.
- 15 Hoyez M.C., Flodrops J.P. & Pegneaux J.C., "Etude d'un Manipulateur de Couche Limite Turbulente en Régime Subsonique Elevé", Rapport de Contrat D.R.E.T. No. 87/24, 1987.
- 16 Lemay J., Provençal D., Gourdeau R., Nguyen V.D. & Dickinson J., "More Detailed Measurements Behind Turbulence Manipulators Including Tandem Devices Using Servo-Controlled Balances", AIAA Shear Flow Control Conference, Boulder, Colorado, March 12-14, 1985, Paper No. AIAA-85-0521.
- 17 Lemay J., Delville J., Garem H. & Bonnet J.P., "Some Detailed Hot-Wire Measurements Behind a Single Manipulator", European Meeting on Drag Reduction, Lausanne, September 1-3, 1986.
- 18 Lemay J., Savill A.M., Bonnet J.P. & Delville J., "Some Similarities Between Turbulent Boundary Layers Manipulated By Thin and Thick Flat Plate Manipulators", 6th Turbulent Shear Flows, Toulouse, September 7-9, 1987.
- 19 Mathews D.C., Childs M.E. & Painter G., "Use of Cole's Universal Wake Function for Compressible Turbulent Boundary Layer", Journal of Aircraft, Vol. 7, N° 2, 1970.
- 20 Mumford J.C. & Savill A.M., "Parametric Studies of Flat Plate, Turbulence Manipulators Including Direct Drag Results and Laser Flow Visualization", FED, Vol. 11, 1984, pp. 41-51.
- 21 Nguyen V.D., Dickinson J., Jean Y., Chalifour Y., Anderson J., Lemay J., Haeberle D. & Larose G., "Some Experimental Observations of the Law of the Wall Behind Large-Eddy Breakup Devices Using Servo-Controlled Skin Friction Balances", AIAA 22nd Aerospace Sciences Meeting, Reno, Nevada, January 9-12, 1984, Paper No. AIAA-84-0346.
- 22 Rashidnia N. & Falco R.E., "Changes in Turbulent Boundary Layer Structure Associated with Net Drag Reduction by Outer Layer Manipulators", NASA Contractor Report No. 178152, 1987.
- 23 Roach P.E., "A New Method of Calculating the Boundary Layer Characteristics Downstream of Manipulators", Turbulent Drag Reduction by Passive Means, R.A.S., 1987, pp. 169-212.
- 24 Savill A.M., Truong T.V. & Ryhming I.L., "Turbulent Drag Reduction by Passive Means: a Review and Report on the First European Drag Reduction Meeting", Lausanne, September 1-3, 1986, to appear in Journal of Theoretical and Applied Mechanics, Gauthier-Villars, 1988.
- 25 Savill A.M., "On the Manner in Which Outer Layer Disturbances Affect Turbulent Boundary Layer Skin Friction" Advances in Turbulence, Springer-Verlag, 1987, pp. 533-545.
- 26 Savill A.M., "Algebraic and Reynolds Stress Modelling of Manipulated Boundary Layers Including Effect of Free-Stream Turbulence", Turbulent Drag Reduction by Passive Means, R.A.S., 1987, pp. 89-143.
- 27 Tenaud C., Coustols E. & Cousteix J., "Modelling of Turbulent Boundary Layers Manipulated with Thin Outer Layer Devices", Turbulent Drag Reduction by Passive Means, R.A.S., 1987, pp. 144-168.
- 28 Veuve M., Truong T.V. & Ryhming I.L., "Detailed Measurements Downstream of a Tandem Manipulator in Pressure Gradients" Turbulent Drag Reduction by Passive Means, R.A.S., 1987, pp. 69-88.
- 29 Westphal R.V., "Skin Friction and Reynolds Stress Measurements for a Turbulent Boundary Layer Following Manipulation Using Flat Plates" AIAA 24th Aerospace Sciences Meeting, Reno, Nevada, January 6-9, 1986, Paper No. AIAA-86-0283.